

# Transient Artifact Reduction using Sparse Optimization

Tong Zhang<sup>1</sup>, Harry L. Graber<sup>2</sup>, Randall L. Barbour<sup>2</sup>, and Ivan W. Selesnick<sup>1</sup>

(1) Dept. Electrical and Computer Engineering, NYU School of Engineering, Brooklyn, NY 11201, USA

(2) Department of Pathology, SUNY Downstate Medical Center, Brooklyn, NY 11203, USA

tz535@nyu.edu, Harry.Grabber@downstate.edu, Randall.Barbour@downstate.edu, selesi@poly.edu

**Abstract:** We address suppression of artifacts in NIRS time-series imaging. We report a fast algorithm, combining sparse optimization and filtering, that jointly estimates two explicitly modeled artifact types: transient disruptions and step discontinuities.

**OCIS codes:** 000.4430, 120.2440

## 1. Introduction

In this work, we address the problem of attenuating artifacts arising in biomedical time-series, such as those acquired using near infrared spectroscopic (NIRS) imaging devices [1]. Our approach is based on the formulation of an optimization problem, which in turn is based on a signal model intended to capture the primary characteristics of the artifacts. We presume only that the artifacts are transient in nature. Specifically, we model the measured time series,  $y(t)$ , as

$$y(t) = f(t) + x_1(t) + x_2(t) + w(t) \quad (1)$$

where  $f(t)$  is a low-pass signal,  $x_i(t)$  are two distinct types of artifact signals, and  $w(t)$  is white Gaussian noise. The ‘Type 1’ artifact signal,  $x_1(t)$ , is intended to model ‘spikes’ and sharp, brief waves; while the ‘Type 2’ artifact signal,  $x_2(t)$ , is intended to model additive step discontinuities. Both types of artifacts are observed in NIRS time series [2].

For the purpose of flexibility and generality, we avoid defining the artifact signals in terms of precise rules or templates. Instead, we define them in terms of sparsity.

1. We define the ‘Type 1’ artifact signal,  $x_1(t)$ , as being sparse and having a sparse derivative. That is,  $x_1(t)$  has a baseline value of zero (i.e., it is sparse) and its derivative is likewise sparse. We use sparsity to encode the transient (brief) nature of the artifacts. Modeling the derivative of  $x_1(t)$  as sparse helps to distinguish it from noise.
2. We define the ‘Type 2’ artifact signal,  $x_2(t)$ , as having a sparse derivative. That is, the derivative of  $x_2(t)$  is mostly zero; hence,  $x_2(t)$  is an approximately piecewise constant signal.

The suppression of both types of artifacts has been addressed in our previous work [3]. Specifically, it was assumed that the measured time series is affected by the presence of either Type 1 artifacts, or Type 2 artifacts, but not both. Two distinct algorithms are described in [3] – one algorithm for each type. The respective algorithms were illustrated on time series acquired using a NIRS system [4] which frequently has artifacts of both types [3, Sect. I-C].

To handle both types of artifacts simultaneously, in this work we develop a new algorithm, denoted ‘Transient Artifact Reduction Algorithm’ (TARA). Complex artifacts often comprise both artifact types, hence the new algorithm performs joint optimization to maximize the effectiveness of the model to better reduce such artifacts. We devise the new algorithm to have high computational efficiency and low memory requirements by constraining all matrices to be banded, so as to leverage fast solvers for banded systems. Moreover, the new algorithm does not require the user to specify auxiliary parameters, such as a step size, which is an improvement in comparison to [3] which requires an auxiliary parameter for the suppression of Type 2 artifacts (i.e., to solve the ‘LPF/CSD’ problem in [3]).

We remark that model (1), where some components are sparse in some sense, is prompted by the approach of morphological component analysis (MCA) in which all components are generally modeled as sparse with respect to distinct (incoherent) transforms [5]. However, the presence of the low-pass component,  $f(t)$ , in (1), differs from conventional MCA approaches. Moreover, compared to MCA, the presence of  $f(t)$  makes the model more realistic for biomedical time-series analysis, and it enhances the prospective sparsity of the remaining components, the sparsity of which is a prerequisite for the applicability of MCA principles.

## 2. Sparse Optimization Formulation

To formulate an optimization problem according to the signal model (1), we write

$$\mathbf{y} = \mathbf{f} + \mathbf{x}_1 + \mathbf{x}_2 + \mathbf{w}, \quad \mathbf{y}, \mathbf{f}, \mathbf{x}_1, \mathbf{x}_2, \mathbf{w} \in \mathbb{R}^N \quad (2)$$

where each vector is a discrete-time sequence. We use the notation  $[\mathbf{v}]_n$  to denote the  $n$ -th component of the vector,  $\mathbf{v}$ .

To formulate the estimation of  $\mathbf{x}_1$  and  $\mathbf{x}_2$  from  $\mathbf{y}$ , we first assume the availability of a low-pass filter,  $\mathbf{L}$ , that satisfactorily estimates the low-pass component,  $\mathbf{f}$ , if it were observed in noise only (i.e., if it were observed without the transient artifacts,  $\mathbf{x}_i$ ). That is, we assume that  $\mathbf{L}$  is available such that  $\mathbf{L}(\mathbf{f} + \mathbf{w}) \approx \mathbf{f}$ . We then define a high-pass filter,  $\mathbf{H} := \mathbf{I} - \mathbf{L}$ . This definition assumes the filter,  $\mathbf{L}$ , is approximately zero-phase; the design of filters for this purpose is discussed in detail in [3]. We then formulate the transient artifact reduction problem as:

$$\{\mathbf{x}_1^*, \mathbf{x}_2^*\} = \arg \min_{\mathbf{x}_1, \mathbf{x}_2} \frac{1}{2} \|\mathbf{H}(\mathbf{y} - \mathbf{x}_1 - \mathbf{x}_2)\|_2^2 + \lambda_{10} \sum_n \phi([\mathbf{x}_1]_n) + \lambda_{11} \sum_n \phi([\mathbf{D}\mathbf{x}_1]_n) + \lambda_{21} \sum_n \phi([\mathbf{D}\mathbf{x}_2]_n) \quad (3)$$

where  $\lambda_{ij} > 0$  and  $\mathbf{D}$  is the first-order difference matrix, i.e., a discrete approximation to the derivative. The three regularization parameters,  $\lambda_{ij}$ , control the relative trade-offs between the two artifact types and the noise. Higher noise variance calls for higher  $\lambda_{ij}$ . The penalty function,  $\phi : \mathbb{R} \rightarrow \mathbb{R}$ , is chosen so as to promote sparsity, for example,

$$\phi_{\text{abs}}(u) = |u| \quad \text{and} \quad \phi_{\log}(u) = \frac{1}{a} \log(1 + a|u|), \quad a > 0 \quad (4)$$

are both suitable. We note that if  $\phi(u)$  is convex (e.g.,  $\phi_{\text{abs}}$ ), then problem (3) is convex and, hence, has a unique minimum value. Therefore, the formulation is well posed and robust. The formulation (3) generalizes and unifies the ‘LPF/TVD’ and ‘LPF/CSD’ problems in Ref. [3].

We have developed a fast algorithm, TARA, for the minimization of (3). In order to attain computational efficiency and avoid algorithm parameters beyond those appearing in the cost function, the algorithm requires several techniques beyond those used in the previous work [3].

## 3. Example

To illustrate transient artifact reduction with TARA (transient artifact reduction algorithm), we apply it to the same time-series data used in Ref. [3] (see Fig. 6 therein). The time series has a duration of 300 sec and a sampling rate of 6.25 samples/sec ( $N = 1900$  samples). The run-time of TARA was 0.36 seconds on a 2013 MacBook Pro (2.5 GHz Intel Core i5) running Matlab R2011a. Figure 1 shows the result of TARA over two sub-intervals to make visible the details of the data and the estimated artifact components. Specifically, TARA produces the signals  $\mathbf{x}_1$  and  $\mathbf{x}_2$  as solutions to (3);  $\mathbf{x}_1$  and  $\mathbf{x}_2$  constitute estimates for the Type 1 and Type 2 artifact signals, respectively. As shown in the figure,  $\mathbf{x}_1$  has a baseline of zero and is sparse, while  $\mathbf{x}_2$  comprises of a few step discontinuities. The total artifact signal,  $\mathbf{x}_1 + \mathbf{x}_2$ , is illustrated in the figure, as is the corrected data,  $\mathbf{y} - \mathbf{x}_1 - \mathbf{x}_2$ . As evident in the figure, the method is able to capture artifact signals with complex waveform shapes. We note that the Welch periodogram of the corrected data shows a prominent peak at about 0.3 Hz (i.e., respiratory rhythm), which is not visible in the periodogram of the raw data due to the presence of artifacts.

## 4. Conclusion

In this work, we describe a method for identifying and suppressing transient artifacts arising in biomedical time series. The method jointly determines both brief amplitude deviations and step discontinuities (Type 1 and 2 artifacts, respectively). The method is non-parametric in the sense that the transients are not modeled through the use of any specified parametric shape. The method is flexible and general enough to encompass a variety of low-frequency background and artifact behaviors, through the tuning of the three parameters,  $\lambda_{ij}$ , and the selection of the low-pass filter,  $\mathbf{L}$ .

## References

1. R. Al abdi, H. L. Graber, Y. Xu, and R. L. Barbour, “Optomechanical imaging system for breast cancer detection,” *J. Opt. Soc. Am. A* **28**, 2473–2493 (2011).
2. T. Fekete, D. Rubin, J. M. Carlson, and L. R. Mujica-Parodi, “The NIRS analysis package: Noise reduction and statistical inference,” *PLoS ONE* **6**, e24,322 (2011).

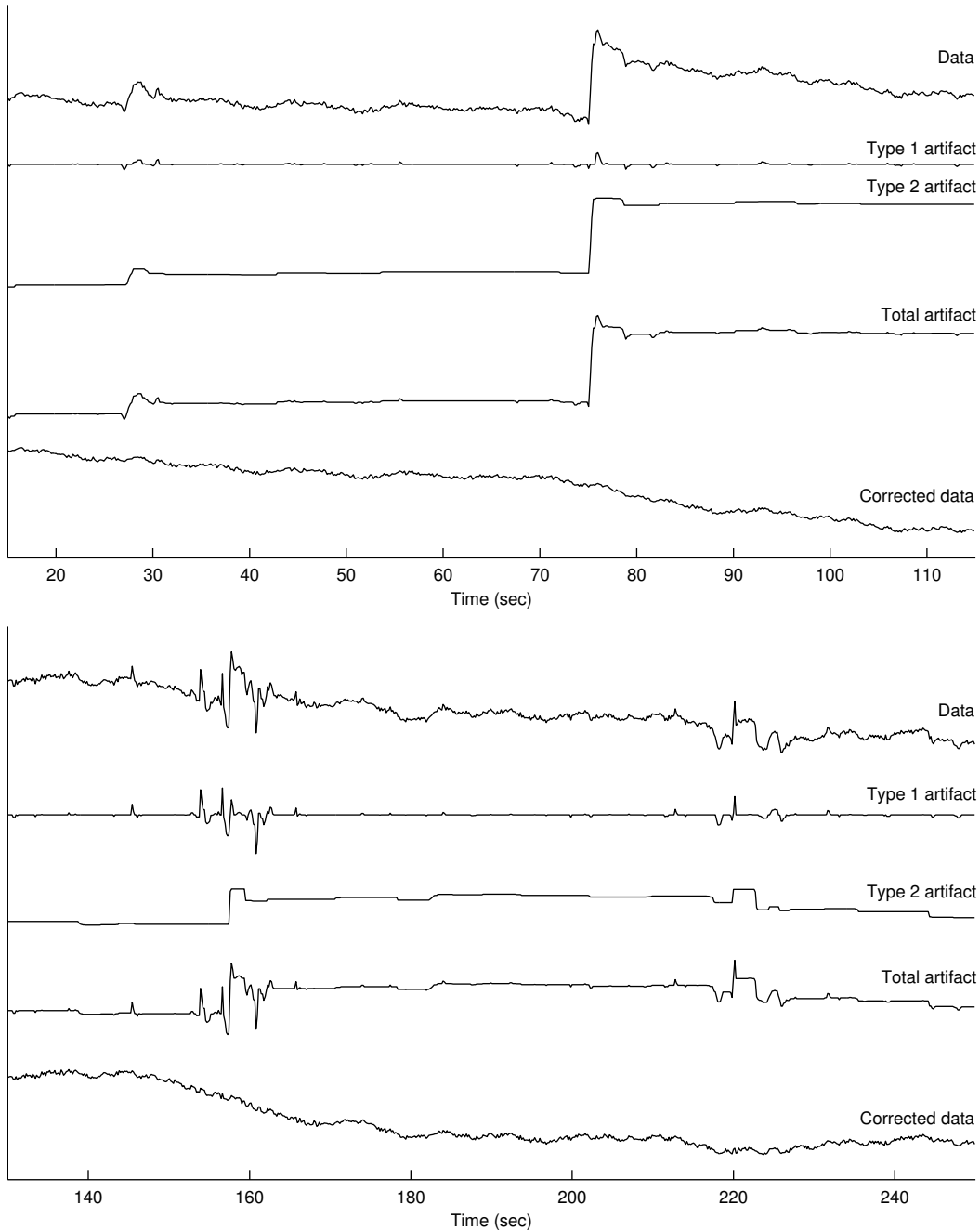


Fig. 1. Illustration of the transient artifact reduction algorithm (TARA).

3. I. W. Selesnick, H. L. Graber, D. S. Pfeil, and R. L. Barbour, "Simultaneous low-pass filtering and total variation denoising," *IEEE Trans. Signal Process.* (2014). To appear. Preprint at <http://eeweb.poly.edu/iselesni/lpftvd/>.
4. J. Mehnert, M. Brunetti, J. Steinbrink, M. Niedeggen, and C. Dohle, "Effect of a mirror-like illusion on activation in the precuneus assessed with functional near-infrared spectroscopy," *J. Biomedical Optics* **18** (2013).
5. J.-L. Starck, M. Elad, and D. Donoho, "Redundant multiscale transforms and their application for morphological component analysis," *Advances in Imaging and Electron Physics* **132**, 287–348 (2004).

This research was supported by the NSF under Grant No. CCF-1018020, the NIH under Grant Nos. R42NS050007, R44NS049734, and R21NS067278, and by DARPA project N66001-10-C-2008.

The authors also gratefully acknowledge Justin R. Estep (Air Force Research Laboratory, Wright-Patterson AFB, OH) and Sean M. Weston (Oak Ridge Institute for Science and Education, TN) for the data used in the example.